Table 1. Reported RBC velocities and frame rates.

Authors	Animal	Method	Average (mm/s)	Range (mm/s)	Frame rate (frames/s)	References
Ma YP, et al	rat	two-slit photometry and cross-correlation	0.75	0.1-2.9	-	[7]
Pawlik G, et al	cat	high-speed microcinephotography	1.50	0.4-3.9	400	[8]
Ivanov KP, et al	rat	intravital microfilming	0.79	0.5-1.5	40	[9]
Chang BL, et al	cat	radioactive microspheres	2.08	0.6-2.9	400	[10]
Yamaguchi S, et al	cat	dual window technique	0.40	0.26-1.1	200	[11]
Villringer A, et al	rat	confocal laser-scanning microscopy	0.60	<1.6	500	[12]
Hudez AG, et al	rat	dual window and cross-correlation	0.61-1.47	0.34-3.15	60	[13-17]
Biswal BB, et al	rat	dual window, cross-correlation	1.00	0.3-1.7	60	[18]
Kleinfeld D, et al	rat	laserscan confocal fluores microscopy	0.77-0.8		62.5	[19,20]
Seylaz J, et all	rat	laser scan confocal fluores. microscopy	0.39		50	[21]
Krolo I, et al	rat	intravital video microscopy	0.41	<1.2	60	[22]
Pinard E, et al	rat	two-photon laser-scanning microscopy	0.51		50	[23]
Schulte ML, et al	rat	intravital video microscopy	0.42	0.17-1.01	60	[24]
Chaigneau E, et al	rat	two-photon laser-scanning microscopy	0.57	0.1-1.5	20	[25]
Hutchinson EB, et al	rat	two-photon laser-scanning microscopy	1.12	0.5-3.5	62.5	[26]

Mean of average velocity was 0.86 ± 0.47 (SD) mm/s.

could be due to differences in methodology, since the experimental animals were the same species and the average RBC velocity under physiological conditions should be consistent.

In our previous communications [27-31], we reported a new high-speed camera laser-scanning confocal fluorescence microscopy system with the custom-made KEIO-IS2 software that tracked RBCs in motion, thus providing quantitative information about their velocity in all blood vessels, including capillaries, across the entire imaged area (or region of interest, ROI) at the layer I of the rat cerebral cortex. This method was very useful not only for rats but also for mice, as the algorithm was both robust and computationally efficient; the method depicts an overview of trajectory directions of all intraparenchymal RBCs in the ROI in 2-D tracking/velocity maps in a sequential manner. Comparison of our method with the 2 photon microscopic method showed that the latter was able to examine intraparenchymal RBC flow and linear density at a few hundred mm depth below the pia, including layer IV, but only in one or two capillaries [19, 32-34]. On the other hand, our method has the advantage to be able to overview many microvasculatures in a wide area, and to detect the dynamic behavior of RBC in high spatio-temporal resolutions for RBC tracking, velocity, and number (density), and capillary recruitment. Concomitant observations can be made on vessels stained with FITC-dextran and astroglia stained with sulforhodamine, together with recordings of EEG, blood gases and other physiological parameters. One limitation to this technique is that observation is restricted to the layer within 100 μm below the pia. Collaboration of the two microscopic approaches is required to provide comprehensive analysis.

The aim of this paper was first to show further feasibility of the KEIO-IS2 method to comprehensively examine the heterogeneity of RBC flow in single capillaries, and then to examine the profiles of velocities of a vast number of RBCs in single capillaries. The RBC velocities were plotted in terms of the frequency distribution function, which was further statistically analyzed for the average RBC velocity in capillaries to distinguish RBCs exhibiting exceptionally high velocities.

Materials and methods

Animal preparation and experimental protocol

Forty-six Wistar rats (mean body weight, 326 ± 31 g) were used with the approval of the Animal Ethics Committee of Keio University. All experimental procedures were in accordance with the university's guidelines for the care and use of laboratory animals. The methods of animal preparation were reported elsewhere [28]. Briefly, each rat was first anesthetized with halothane followed by an intraperitoneal injection

of 10 % urethane (1 ml/100g body weight); rats were fixed to a head-holder and a cranial window of approximately 4 mm was opened in the left side of the skull at the parieto-temporal region of the cerebral cortex. The dura was carefully removed and the exposed cortex was covered with a cover slip to prevent it from drying up. A femoral artery and a femoral vein were catheterized to monitor systemic arterial blood pressure (SABP) and intravenously inject various solutions, respectively.

After selecting an appropriate capillary-rich ROI in the cerebral cortex 50-80 μm below the pia, 0.5 ml of fluorescein isothiocyanate (FITC)-labeled RBC suspension, prepared beforehand according to Seylaz et al. [21], was injected into the bloodstream through the venous catheter. We found that the final concentration in the circulating blood was approximately 0.4 % of whole body blood RBC. At the end of experiments, 0.2 ml of 0.25 % FITC-dextran (70 kD) was intravenously injected to stain vessels to confirm capillaries by overlapping results with RBC tracking maps, retrospectively.

In all experiments, SABP was routinely recorded via a strain gage transducer connected to the femoral arterial catheter on a personal computer (PC) with Acknowledge software (MP 100 WS). In 4 rats taken up at random, physiological parameters were measured with a blood gas analyzer (Rapidlab, Siemens, Tarrytown, NY, USA) after sampling arterial blood through arterial catheter to confirm this experimental condition to be within physiologically normal range.

Measurements of RBC velocity

The equipment assembly of the high-speed camera laser scanning confocal fluorescence microscope and the image analyzing system were as follows: the rat brain was fixed on the stage of the microscope with an objective lens (LU Plan EPI SLWD 20x NA=0.35) or a water immersion lens (Plan Fluor 20x W NA=0.50, Nikon, Tokyo, Japan), a multi-beam confocal scanning unit (CSU22, Yokokawa, Tokyo, Japan), an image intensifier (C6653MOD-N, Hamamatsu Photonics, Hamamatsu, Japan), and a MotionPro high-speed camera (Model 500) with a digital imaging system with the MiDAS program file (RED-Lake, San Diego, CA, USA). This set-up enabled us to acquire images of FITC-labeled RBCs excited by an argon laser (λ= 488 nm, Melles Griot, Carlsbad, CA, USA) at 125, 250, and 500 frames/s (fps) with shutter speeds of 1/125, 1/250 and 1/500 seconds, respectively. The image signal system was switched to either the high-speed camera or to a conventional video camera (30 fps, DCR-PC100, Sony, Tokyo, Japan) as shown in **Fig. 1**.

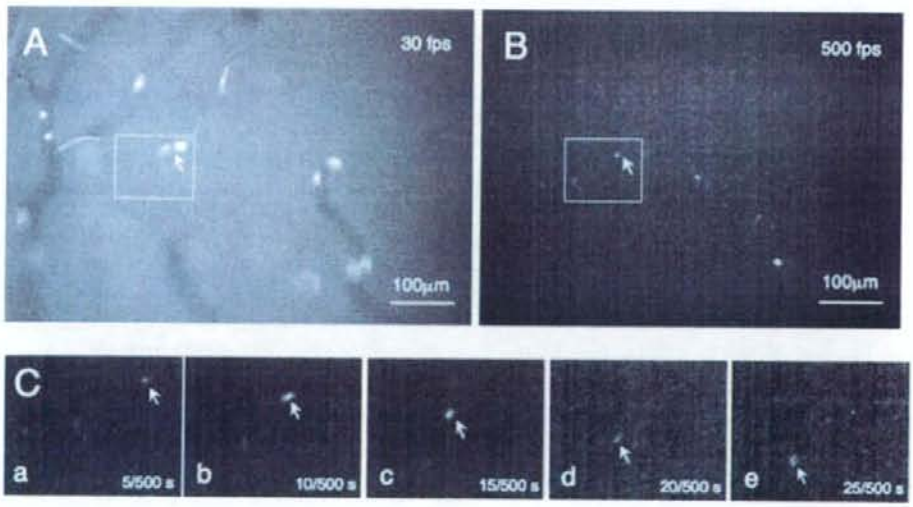

Fig. 1 (**A**) A microphotograph taken from a videotape recorded at 30 fps. (**B**) A microphotograph taken from a video clip recorded at 500 fps in an avi file in the same ROI as **A**. Scales are shown in the bottom right of the figures. (**C**) Enlarged sequential images showing the movement of the RBC in the inset of A and B. Images were captured every 0.01 second, and the continuous translocation of the RBC is indicated by white arrows (**a-e**). The locations at x-y coordinates of the centroids of all RBCs are stored in the computer used for the following calculations. Notably, the shape of the FITC-labeled RBCs tended to appear elongated at 30 fps, and round at 500 fps.

The high-speed camera was able to adjust frame rate and shutter speed separately, and in these experiments, the frame rate and shutter speed were adjusted to be the same. Images acquired with the high-speed camera system were stored in discrete sequential video clips, which were transferred to a PC and processed in a MATLAB® (The Math Works, Inc., Natick, MA, USA) environment using application software (KEIO-IS2) developed in our laboratory [27]. Details of the software were previously described [28]. Briefly, the software was customized by setting several parameters; gray-level threshold was automatically applied to each frame to differentiate FITC-labeled RBCs from the background, all particles having 8 connected pixels were recognized as RBCs, scale was set at 1 μm/pixel, maximum RBC displacement distance from the original position was set at 20 μm, and the minimum number of frames of RBC movement as three. These settings were determined based on trial and error, and confirmed to be appropriate by the method validation.

The images of the selected video clip were automatically analyzed for frame-by-frame movements of all RBCs to yield an RBC tracking map (T map; **Fig. 2**), frame-by-frame dislocation (distance) multiplied by frame rate to yield an RBC velocity map (V map: **Fig. 3A**) and accumulation of RBC to yield an RBC number map (N map; **Fig. 3B**) together with their color scales. In the RBC tracking map (**Fig. 2**), RBCs were automatically labeled in the order of appearance by different colors with identification numbers. All RBC velocity data with the identification numbers were then transferred to a spreadsheet (Microsoft Excel) for statistical analysis.

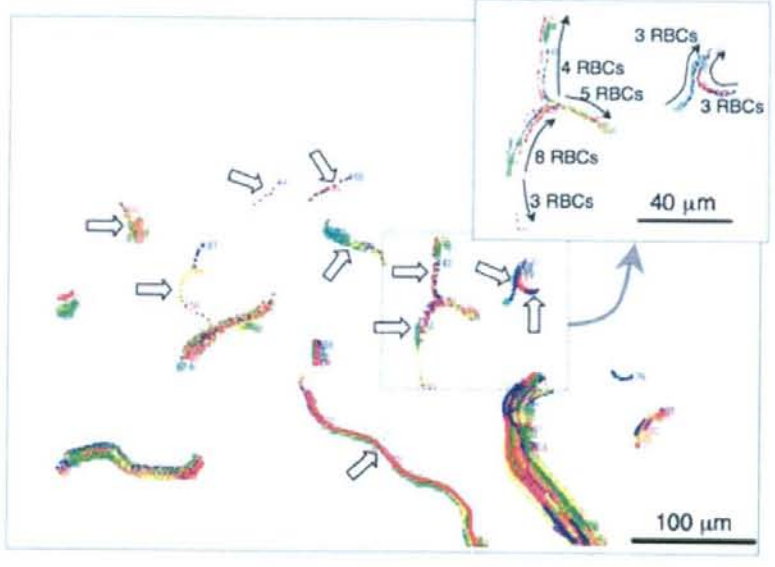

Fig. 2 FITC-labeled RBCs in the same ROI as **Fig. 1** during a period of 10 second (5000 frames). Sequential dots and numbers in specific colors indicate frame-by-frame movements of RBCs in the microvessels. The distance between the same color dots in a sequence indicates movement (distance) of each RBC during 1/500 second. From the distance and the frame rate, the velocity of the RBC at the given location in the vessel at the given time was calculated. Open arrows indicate capillaries confirmed by FITC-dextran staining, revealing that low RBC velocities do not necessarily indicate capillaries and heavy RBC traffic does not necessarily indicate large vessels. In the inset at the upper right corner, enlarged RBC trackings in a branching capillary are shown.

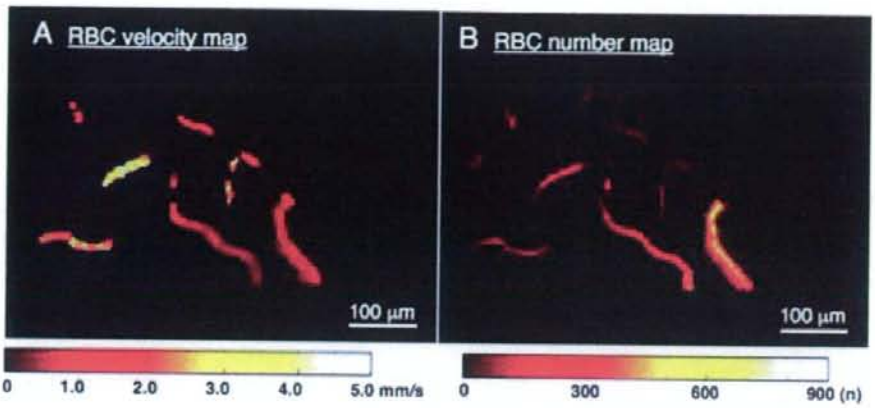

Fig. 3 (A) RBC velocity map and (B) RBC number map calculated from the video clip taken at 500 fps from Fig. 2. Scales are shown at the bottom of the figures. Calculated velocities of all RBCs were transferred to a spreadsheet for further analysis (see text for further explanation).

Identification of capillaries

We defined single capillaries as FITC-dextran-stained vessels with a diameter less than 10 μm, based on other reports [26, 35]. However, we noticed that the amount of FITC-dextran required to clearly visualize the capillary wall not only increased the background brightness, which sometimes disturbed the detection of FITC-labeled RBCs, but also caused microvascular derangement [28]. Therefore, the confirmation of capillaries by this approach was conducted in only 10 rats at the end of the experiments. In the remaining experiments, capillary populations were separated by cluster analysis based on our criteria that single-file tracking of RBC represented a single capillary, which was confirmed based on the initial experiments with the 10 rats.

Statistics

Data in text and figures are presented as mean ± standard deviation (SD). Non-paired student's *t* test was performed to assess statistical significance. The significance level was set at $p<0.01$.

As shown later, the frequency distribution function of velocities was not symmetrical, and rather was skewed to the lower velocities. With the assumption that some RBC velocities could belong to a non-capillary group or more explicitly to thoroughfare channels, we attempted to exclude such extraordinary high velocities that were sufficiently far from the main population of velocities in capillaries. We tested the utmost outlying value X statistically at a level of $p<0.01$ based on $(\bar{x}-X)/s$, where $\bar{x}$ is the mean, and s the standard deviation [36]. We excluded the outlying value from the parent population of velocities, and then re-calculated the mean and SD of the remaining velocities. We repeated the calculation to exclude the next most outlying values. This procedure was repeated for outlying values until the probability (p-value) reached 0.01.

Analysis of frequency distribution function

We plotted RBC numbers (n) against velocities (V_m, where m=0.2, 0.4, 0.6 ... mm/s) obtained at each frame rate. Individual RBC numbers were made dimensionless by dividing by total number of rat so that the frequency distribution function, $h(V_m)$, in single capillaries was obtained.

Using all velocity values in $h(V_m)$, we estimated the relative amount of oxygen delivered by arterial blood (D) to the tissue per unit time (10 seconds): $D = \sum_{*}^{***} c\ n_{(V)}\ f_{(V)}$, where c was the arterial oxygen content, n the passed RBC number at V_m, and f the flow linearly related to velocity ($f_{(v)} = \alpha V_m$, where a is a constant). RBCs contributing to linear hematocrit in single capillaries were included in n as values independent from velocities. Theoretical calculation was further performed on oxygen extraction (E) based on the classic Crone-Renkin equation [37]. Oxygen extracted at the capillaries was expressed as: $E = 1 - e^{-PS/f}$, where P is a constant related to the permeability and S corresponds to the multiple of capillary surface area and length [38]. The equation implies that gas in fast flowing blood is less extracted, with little exchange

in the tissue and a large amount of oxygen left unused in the venous blood. When E was subtracted from D, the amount of shunting or unextracted blood could be obtained.

Results

General observations

Physiological conditions of the rats remained unchanged during RBC velocity measurements: the average SABP (n=46) was 102±15 mmHg at the beginning of experiments, with little fluctuation thereafter, within 2.5±10.3 mmHg. Physiological parameters (n=4) were within normal limits: hematocrit, 56.5±2.7 %; arterial PO_2, 105.6±5.1 mmHg; arterial PCO_2, 41.2±2.6 mmHg; and arterial pH, 7.38±0.04.

Typical microphotographic images of RBC movements in the microvasculature are shown in **Fig. 1 A** and **B**. **Figure 1A** is a frame taken from a videotape at 30 fps that ran continuously throughout the experiment, with only occasional interruption for data acquisition from high-speed camera recording (125-500 fps) of the same ROI. **Figure 1B** is a frame taken from the video clip of FITC-labeled RBCs with the high-speed camera at 500 fps. The intravenously administrated FITC-labeled RBCs are seen as mostly elongated particles at 30 fps compared to the bright round appearance at 500 fps. Elongated or round RBCs were registered at their centroids in x-y coordinates at each frame. RBC movements were followed up by images captured sequentially over time, taken from the inset in B every 0.01 second (**Fig. 1C, a-e**). The RBC indicated by a white arrow moved 150 μm in 1/20 s, and the velocity was therefore calculated as 3 mm/s (150 μm x 20/s). **Figure 2** is the RBC tracking map (T map) obtained from 5000 frames (10 seconds) of a video clip used for **Figure 1B.** As defined in the previous paper [28], the data subset of the video clip was expressed as $[5000_{1\text{-}5000}, 500]_{67\text{-}1}$ (which represents 5000 frames from the 1st frame to the 5000th frame clipped from data set 1 of experiment number 67 acquired at 500 frames/s). RBCs were automatically numbered in the order of appearance, and RBCs in capillaries were indicated by open arrows while other RBC tracking files indicated RBCs in non-capillary vessels such as arterioles and venules. The RBC tracking map (T map) thus represents all RBCs in arterioles, capillaries and venules and contains almost all information necessary for the microcirculatory analysis, such as RBC velocity from the distance moved during a frame interval (1/500 second), RBC number, direction of RBC movement, linear hematocrit, and capillary number. Thus, the T map could be termed the representative "face" of the microcirculatory status at the location in the given moment. An enlarged RBC tracking map of a branching capillary from **Fig. 2** is shown in the upper right corner. The directions of the movements of numbered RBCs were confirmed by playing back the original video clips in slow motion. It should be noted that RBCs distributed irregularly to daughter capillaries, and that the movements along the capillaries were not smooth. The RBC velocity map (**Fig. 3A**) and RBC number map (**Fig. 3B**) were processed with the KEIO-IS2 from the $[500_{1\text{-}500}, 500]_{67\text{-}1}$ data subset. Note the similarity of their contours to the T map in **Fig. 2**; however, the images represent sequences of varying individual RBC velocities and summed number of RBCs at the same location during 1 second.

RBC velocity fluctuations

The above data of RBC velocities included all RBCs in arterioles, capillaries and veins. To focus on RBC velocities in single capillaries, vessels were stained with FITC-dextran and those with a diameter of less than 10 μm were identified as capillaries. RBC velocity in capillaries ranged from 0.12 to 4.19 mm/s, and the average velocity was 1.38 ± 0.3 mm/s (mean ± SD), fluctuating within a range of 0.90 and 1.93 mm/s at 250 fps in 10 rats (**Table 2**). By comparison, RBC velocity in non-capillary vessels varied more widely than in capillaries, as non-capillary vessels included various types such as venules and arterioles. **Figure 4A** shows all RBC velocities, both in capillaries and non-capillaries, in the order of appearance from the data set $[250_{750\text{-}1000}, 250]_{17\text{-}4}$. **Figure 4B** shows RBC velocities arranged in the order of magnitude of velocity. The RBC velocities in capillaries were not necessarily low, implying that capillaries could not be characterized as such based on only low RBC velocity.

Frame-rate dependency

As shown in **Fig. 5,** the average velocities of RBCs in capillaries increased with increasing frame rate: 0.93 ± 0.28 mm/s at 125 fps (n=6), 1.38 ± 0.30 mm/s at 250 fps (n=10) and 2.21 ± 0.73 mm/s at 500 fps (n=37). The differences were statistically significant between each pair of the 3 groups ($p<0.01$). The frame-rate dependent increase of RBC velocity occurred even though the observations were made in

the same ROI. In 4 rats, the RBC velocities were determined at 3 frame rates in the same ROI, in which the average velocities had a tendency to increase with increasing frame rate: 1.00 ± 0.32 mm/s at 125 fps, 1.32 ± 0.44 mm/s at 250 fps and 1.94 0.56 mm/s at 500 fps. The number of detected RBC in capillaries also increased with increasing frame rate: 42 ± 30 at 125 fps, 85 ± 47 at 250 fps and 117 ± 77 at 500 fps. The average RBC velocity in non-capillary vessels (arterioles and venules) also increased with increasing frame rate between each group ($p<0.05$). Velocities both in capillaries and non-capillary vessels tended to be distributed in a similar pattern, so that it was not possible to discriminate between the types of vessels based on velocity values alone.

The total number of RBCs in capillaries obtained was 4311 RBCs at 500 fps (n=37 rats), 849 RBCs at 250 fps (n=10 rats) and 250 RBCs at 125 fps (n=6 rats). The frequency distribution functions of velocities at each frame rate are shown in **Fig. 6**. The ranges of velocity were 0.15 to 9.40 mm/s at 500 fps, 0.12 to 4.19 mm/s at 250 fps and 0.07 to 1.93 mm/s at 125 fps. The maximum frequencies were shown around 1 mm/s at any frame rates. 62 %, 77 %, and 82 % of the RBCs in capillaries detected at 500, 250 and 125 fps, respectively, exhibited velocities that fell within a small range of 0.4 to 2.0 mm/s. It should be noted that the higher velocities could only be detected at higher frame rates, and these high velocity RBCs were missing when lower frame rates were used for analysis, as the RBCs moving at higher velocity were too fast to be captured until a higher frame rate was used for detection.

Figure 7 shows tracking of RBCs in the microvasculature in the same ROI at various frame rates. RBC numbers increased with frame rate, indicating that more RBCs were captured at 500 fps, and/or some RBCs were missing at lower frame rates, even though the same number of RBCs must be flowing in the actual microvasculature. Analysis of three specific capillaries (1, 2 and 3) showed that the RBC velocities differed, as shown by scattergrams (**D, E** and **F**). We found that appearances of RBCs and velocities in single capillaries fluctuated over a 10 sec period, but that the range of fluctuation was similar at any frame rate examined in each capillary. Velocity in a high flow capillary (**Fig. 6E**) was obtained only at higher frame rates because of the detection limit at the low frame rate. In contrast, velocity in a slow flow capillary was detected at any frame rate (**Fig. 6F**). This indicated that in some capillaries, RBCs moved too quickly to be detected by the camera at a low frame rate.

Table 2. Average and range of RBC velocities and numbers of RBCs in capillaries and in non-capillaries.

Rat No.	Capillaries Average velocity (mm/s)	Range (mm/s)	n	Ratio (%)	Non-capillaries Average velocity (mm/s)	n
1	1.32±0.53	0.21-2.97	86	15.2	1.30± 0.85	481
2	1.35± 0.68	0.12-3.61	141	34.4	2.77± 0.98	269
3	1.64± 0.77	0.42-3.70	98	19.5	2.34± 1.19	405
4	1.44± 0.64	0.48-3.36	101	14.5	2.84± 0.71	595
5	1.13± 1.10	0.19-3.79	33	6.6	2.39± 0.85	465
6	1.67± 0.88	0.17-4.02	131	17.4	1.62± 0.80	621
7	1.29± 0.79	0.26-2.89	38	16.2	2.06± 1.07	196
8	1.17± 0.52	0.48-4.12	65	30.4	2.62± 0.70	149
9	0.90± 0.38	0.18-2.31	144	32.5	1.23± 0.64	299
10	1.93± 1.14	0.37-4.19	12	11.1	2.77± 0.70	96
Mean	***1.38± 0.74***		***84.9***	***19.8***	***1.93 ±0.85***	***357.6***

Values are means ± SD. Numbers (**n**) represent detected RBC numbers flowing in capillaries and in non-capillaries. Ratio represents percentage of RBC numbers in capillaries to total number of RBC. Video clips used for calculation were obtained at frame rate of 250 fps and shutter speed of 1/250 second for 10 second.

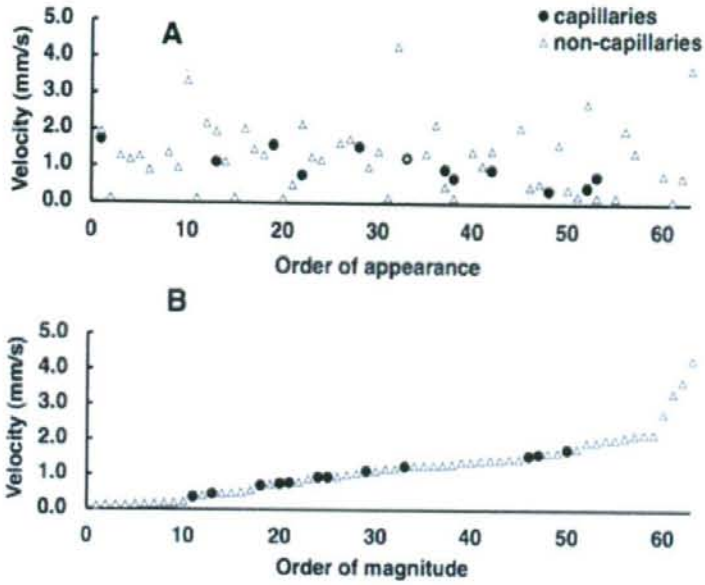

Fig. 4 Heterogeneity of RBC movements in single capillaries and non-capillaries. The closed circles indicate RBC velocities in capillary, whereas the open triangles indicate RBC velocities in non-capillaries. RBCs assessed in the order of appearance from images obtained from a ROI at 250 fps for one second. In the upper panel **(A)**, 13 RBC tracks were identified in capillaries among the total of 63 detected RBC tracks. The lower panel **(B)** shows re-plotting of the above data in the order of magnitude of velocity, implying that low velocity is not necessary for RBCs to be in single capillaries. RBCs of much lower velocity exist in venules, and those with faster velocities are mostly in arterioles.

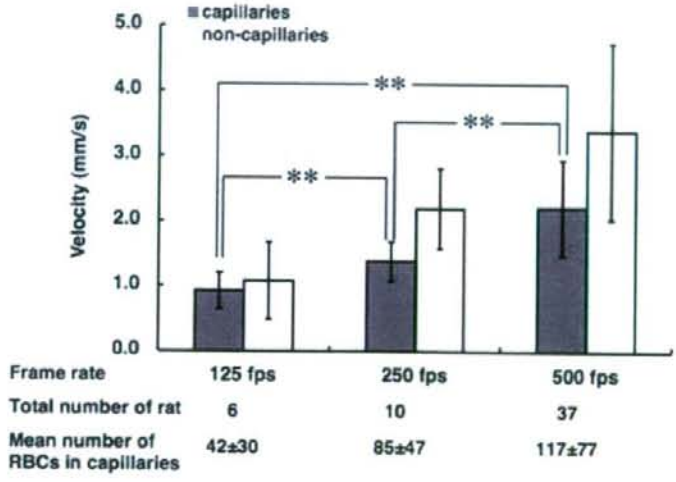

Fig. 5 Apparent dependency on frame-rate of average RBC velocities in capillaries (gray column) and non-capillary vessels (open column). Velocities were obtained at frame rates of 125 (n=6), 250 (n=10) and 500 fps (n=37). Values are represented as mean ± SD. Asterisks (**) show statistically significant difference with $p<0.01$ between paired 2 groups.

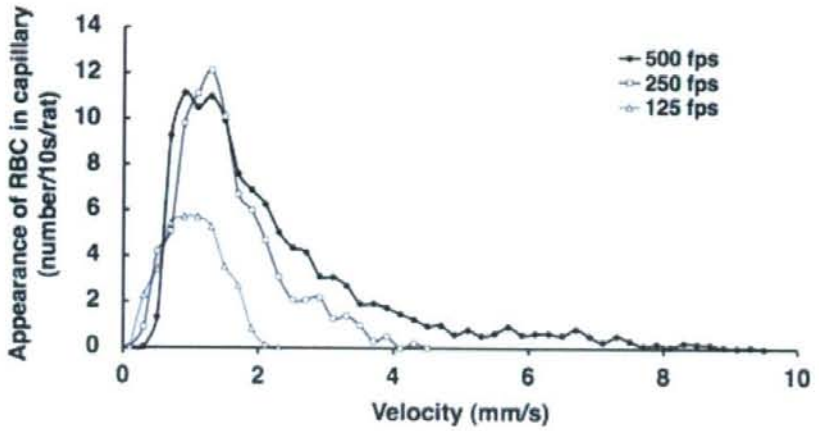

Fig. 6 Frequency distribution functions of velocities obtained at 500 fps (closed circle, n=37), 250 fps (open square, n=10) and 125 fps (open triangle, n=6) for 10 s. RBC velocities were stratified every 0.2 mm/s from 0 to 10 mm/s. The coordinate (total RBCs in each velocity range) was normalized by the number of rats. Displayed curves represent probability of RBC appearance at given velocity.

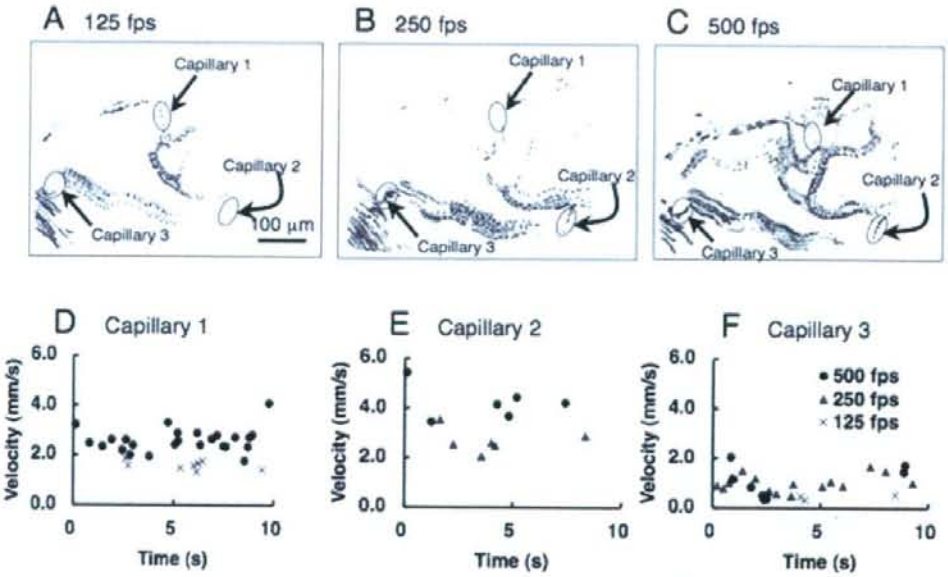

Fig. 7 Variations in T maps (different "faces") of the same ROI at 125 fps (**A**), 250 fps (**B**) and 500 fps (**C**). (**D**, **E**, **F**) Calculated velocities plotted against time, showing changes in velocity over time in single capillaries **1**, **2**, and **3**. Average velocities in each capillary were 2.35±0.61 (**A**), 3.46±0.99 (**B**) and 0.93±0.47 mm/s (**C**). Notably, high velocity RBCs are missed at lower frame rates as shown in **E**.

Velocity fluctuation in single capillaries

Capillaries in which RBCs were detected at least 5 times were selected from the velocity data obtained from the images recorded at 500 fps in 37 rats (**Fig. 8**), resulting in a total of 161 capillaries with 2,379 RBCs passing through the capillaries. We calculated mean velocities of RBCs for the individual capillaries and the mean values were plotted with small bars, with all velocities as small dots. The mean and standard deviation of the individual mean velocities in single capillaries was 1.96±1.26 mm/s, which is shown by a dotted line in **Fig. 8**. The average of the individual fluctuations (SD) of RBC velocities in single capillaries was 0.59±0.38 mm/s. RBC velocities continually fluctuated within a limited range of velocities specific to individual capillaries. In other words, RBC velocities in single capillary varied within a similar range of approximately 0.6 mm/s, as shown above. **Figure 8** represents all velocities in single capillaries, which contain RBCs with extraordinarily high velocities. When the Grubbs' outlying test [36] was employed, RBC velocities over 6.5 mm/s were excluded from the main population ($p<0.05$). After excluding these extraordinary high flow values, the final mean RBC velocity in capillaries was 1.90±0.58 mm/s.

We then investigated the relationship between RBC velocities in single capillaries and the length of the capillaries. A total of 161 capillaries were identified and analyzed at 500 fps, 38 capillaries at 250 and 17 capillaries at 125 fps (**Fig. 9**). The length of the capillaries in the optically sliced thin layers ranged from 30 to 300 μm in length. Calculated velocities tended to be lower when capillaries were longer at any frame rates, but there was no statistically significant correlation between capillary length and RBC velocities (r=-0.07 at 500 fps, -0.08 at 250 fps and -0.18 at 125 fps). The correlation coefficient of the total RBC velocity and corresponding capillary lengths was -0.07.

Frequency distribution function

The total number of RBCs in capillaries was 4,311 among the total 21,078 RBCs detected at 500 fps for 10 seconds in the ROI of 37 rats. The frequency distribution function of RBC velocities in capillaries is shown in **Fig. 10** (closed circles). Velocities were stratified by 0.5 mm/s and indicated as a relative value to the maximum value as 10. The average velocity was 2.05 ± 1.59 mm/s, including extraordinary high flow RBCs. When all velocities were tested for an outlying group by the method reported by Grubbs [36], an RBC velocity over 6.5 mm/s was found to be statistically significantly higher than the main population ($p<0.01$). Such a high-flow capillary was considered to be a thoroughfare channel. After excluding these extraordinary high velocity values, the mean velocity in capillaries was calculated as 1.89 ± 1.32 mm/s.

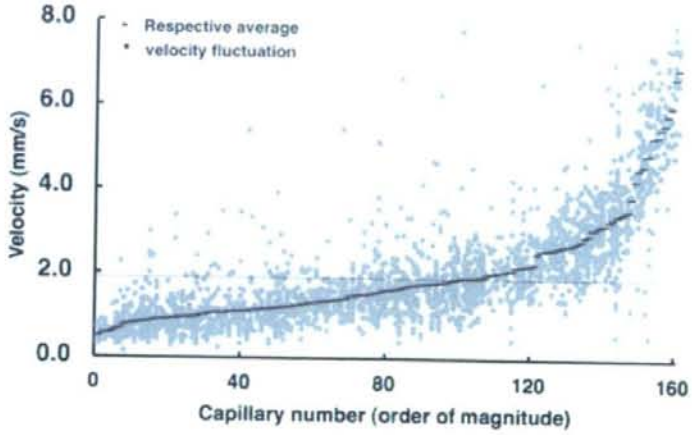

Fig. 8 Fluctuation (small dot) and respective averages (small bars) of RBC velocities in individual capillaries. One hundred and sixty one capillaries, in which RBC tracks were detected 5 or more times (recorded at 500 fps for 10 seconds), were selected in 37 rats and ranked in order of their average velocities. All fluctuating velocities were plotted against the rank. The mean (1.96 mm/s) of individual averages is shown by the dotted line. It should be noted that velocities over 6.5 mm/s differed from the main population in a statistically significant manner ($p<0.05$).

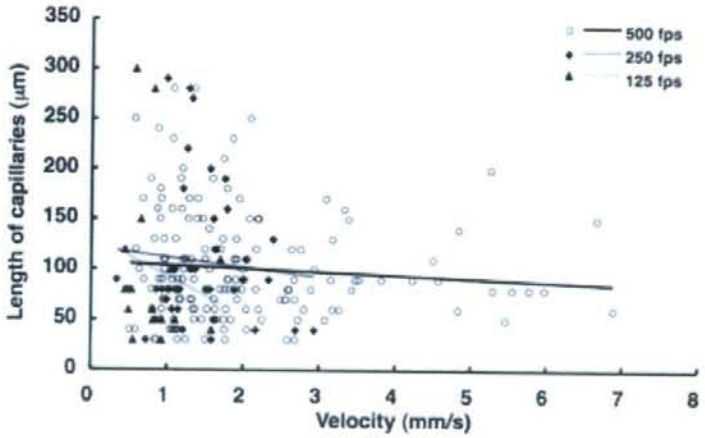

Fig. 9 Relationship between the RBC velocity in single capillaries and capillary length. Shapes represent different frame rates (open circle: 500 fps; gray rhombus: 250 fps; gray triangle: 125 fps). There was no statistically significant correlation between velocity and length (r=-0.07).

The amount of oxygen delivered to the tissue by arterial blood (**D**) was calculated and plotted as shown in **Fig. 10** (open squares). Theoretical extraction of oxygen (**E**) was also plotted in distribution function as shown in **Fig. 10** (open triangles). Broad calculation of the shunting blood over the total arterial blood volume flow yielded 42 % of the blood in the venous system without gas exchange under physiological conditions (**Fig. 10,** shadowed area).

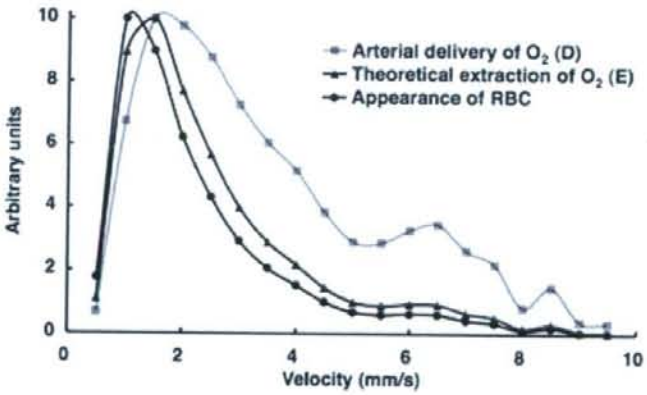

Fig. 10 Frequency distribution functions of RBC velocities in single capillaries. Total appearance of RBCs (closed circle), amount of delivered oxygen by the artery (open square) and amount of extracted oxygen (open triangle). Each plot is shown dimensionless as a normalized value to the maximum 10. A total of 4,311 RBC velocities were obtained at 500 fps for 10 s from 37 rats, and were stratified for every 0.5 mm/s. Velocities over 6.5 mm/s were statistically significantly different from the general population ($p<0.05$) (see text for explanation of the exclusion technique). The shadowed area shows the difference obtained by subtraction of the extracted oxygen from delivered oxygen by the artery, representing reserved oxygen directly passing to the venous system without gas exchange.

Discussion

RBC velocity in single capillaries

Our results presented here demonstrate that the movement of RBCs in single capillaries is not constant, but rather varies over time. The fluctuation of RBC flow became more prominent when video images were obtained with a high-speed camera, although the target microcirculation in situ is most likely the same as the RBCs assessed with the low-speed camera. In addition, we found a robust increase in RBC velocity when measured with a high frame rate compared to measurements with a low frame rate. This tendency is consistent with previously reported experiments in the literature. We plotted the RBC velocities in **Table 1** are plotted against frame rate, excluding the data of Hudetz et al. [14], Krolo et al. [22] and Villringer et al. [12] who only used velocities lower than a certain threshold for capillaries. Then, a broad frame-rate dependency of the increase in RBC velocity was observed, as shown in **Fig. 11**. This indicates that the rapidly moving RBCs are detected only when a high-speed camera is used for analysis. The critical nature of this finding strongly warrants a reinvestigation into the mechanism of RBC velocity and, accordingly, past studies on RBC velocities should be reappraised.

Consider, for example, a long capillary **A** (100 μm) and a short capillary **B** (30 μm), in which RBCs flow at a velocity of 2 mm/s (**Fig. 12**). When analyzed at 60 fps, a RBC in capillary **A** would be recorded as moving 33 μm in the subsequent frame (1/60 second later) and could be captured 4 times within 1/20 second. In comparison, when recorded at 500 fps, the RBC would be recorded as moving 4 μm in the subsequent frame in 1/500 second and could be captured 26 times within 1/20 second. On the other hand, the RBC in capillary **B** recorded at 60 fps could not be measured since the RBC would be detected only once in the short capillary as it moves away in the next frame (33 μm apart during 1/60s moving through the 30 μm capillary). However, when the measurement is obtained at 500 fps, the RBC is detected seven times since it moves 4 μm per 1/500 s through the 30 μm capillary. Thus, a rapidly moving RBC could be recognized even in the short capillary at 500 fps.

RBC velocities in cerebral capillaries were reported in the range from 0.39 to 2.08 mm/s, with an upper limit of 3.9 mm/s as shown in Table 1. According to Ivanov et al. [9] and Hudetz et al. [15], 63 % and 65 % of obtained RBC velocities fell in the range of 0.5 to 1.5 and 0.5 to 1.8 mm/s, respectively. Hudetz et al. defined a 'capillary' as one with RBCs exhibiting a resting velocity of less than 1.2 mm/s, in addition to the vessel diameter and morphological considerations [14]. In the present study, 62 % of RBC velocities in capillaries exhibited within a small range of 0.4 to 2.0 mm/s, and 46 % was below 1.2 mm/s when recorded at 500 fps. This apparently low ratio of slow RBCs is explained by the high numbers of faster RBCs detected in this study, which compresses the ratio to a relatively low level.

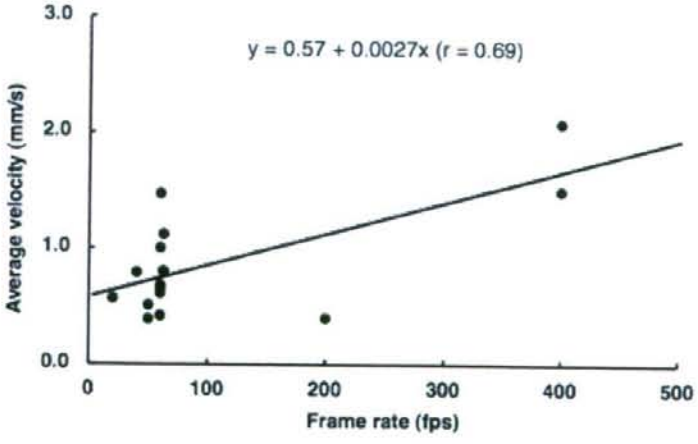

Fig. 11 RBC velocity (y-axis) and frame rate (x-axis) plot of the data shown in **Table 1**. Note that the tendency of RBC velocity to increase with frame rate. The regression line is y=0.57 + 0.0027x (r=0.69).

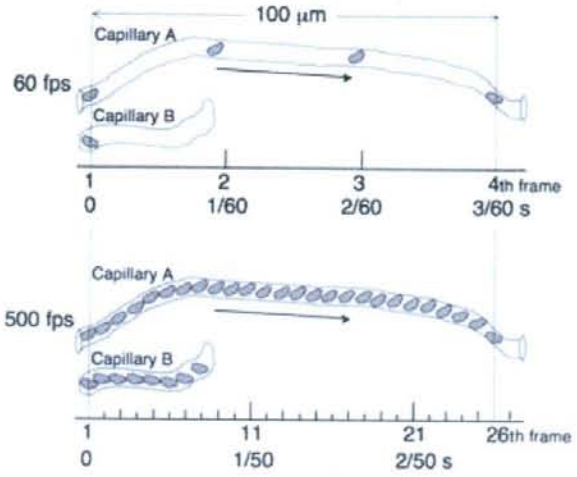

Fig. 12 Hypothetical model of long capillary **A** (100 μm) and capillary **B** (30 μm) in which RBCs flow at a velocity of 2 mm/s recorded at 60 fps (top panel) and 500 fps (bottom panel). Note that in capillary **B**, the RBC has moved away in the next frame and is not detected.

The maximum velocity, which had been limited in traditional frame-by-frame analysis of video recordings to about 2 mm/s, was raised to 20 mm/s using an electronic shuttering of an intensified charge-coupled device camera with a shuttering rate of 1 MHz [39]. However, the system was limited to *in vitro* and the upper limit of the calculated velocity was much lower with a frame rate of less than 500 Hz *in vivo*. Japee et al. developed MASCOT (measurement and analysis system for capillary oxygen transport), which enabled the automatical analysis of individual RBC movement through capillary networks and oxygenation of blood in hamster cheek pouch retractor muscle [40, 41]. However, the maximum measurable velocity was approximately 2 mm/s, and the maximum value of calculated velocity in capillaries was approximately 0.5 mm/s, likely due to the use of a conventional videocassette recorder with a frame rate of 30 fps. In the present study, the upper limit of measurable velocity is 10 mm/s. Therefore, the present method using a high-speed camera is a better method to automatically measure the wide range of RBC velocity and movement, especially for analysis of the vast number of moving RBCs in the microvasculature at a high velocity *in vivo*.

Heterogeneity of RBC velocities

As stated above, the present study demonstrated a marked heterogeneity of capillary RBC flow even in the resting state (**Figs. 4, 7** and **8**). This observation is consistent with previous studies [8, 19, 35]. When we focused on a single capillary, the direction of flow and average rate of RBC perfusion are comprehensively related to the pressure head of the capillary, but local heterogeneity must be, at least in part, due to dynamic variation of neuronal activity and related capillary changes in space over time. Fluctuations in RBC velocity and RBC flow cessations over a short period were observed in some capillaries (see **Fig. 7D, E, F**), confirming observations by Hudetz [42]. The heterogeneity of capillary perfusion of RBC suggests that many capillaries are not maximally utilized under resting conditions. In capillary shift from a heterogeneous flow at rest to a more homogeneous flow during stimulation, the major changes in high-flow RBC perfusion accompanied by a reduction in number of low-flow capillaries [12]. According to the concept of capillary recruitment, these low-flow capillaries may be functionally reserved capillaries. Schulte et al. reported that capillaries with a low resting velocity showed a greater response to electrical stimulation than those with a high resting velocity, and that the shape of the velocity distribution changed as the mean RBC velocity increased with stimulation [24]. Analysis with our method may provide key insights into understanding the variable capillary flow responsibility.

Oxygen supply and blood perfusion

Path length of capillaries and transit time of RBC and plasma are important determinants of capillary gas and nutrient exchange. The length of the capillaries depended on the thickness of the optically sliced layer. Since the RBC tracking map cannot reflect RBC movement along the z-axis, the lengths in the present study may be underestimated. However, the range is almost consistent with that reported by Pinard et al. [23]. Hudetz et al. reported RBC transit times between 100 and 300 ms and flow path lengths between 150 and 500 μm in the same capillary network [13, 43]. In the present study, the length of most capillaries was between 30 and 300 μm (63 % of the capillaries were less than 100 μm) and the calculated RBC transit times through the capillary was 9 and 531 ms (77 % of the capillaries showed transits of less than 100 ms), where the capillary length was measured as the distance of RBC movement on the two-dimensional RBC tracking maps.

Cerebral oxygen supply is regulated mainly by a change in the rate of perfusion and much less by an alteration in the diffusion distance of oxygen. Hudetz et al. reported a proportional relationship between cerebrocortical blood flow and oxygen consumption in the normal physiological range of functional activation, with capillaries defined by a resting velocity of less than 1.2 mm/s [44]. In this study, we showed that a relationship between RBC velocity and theoretical extraction of oxygen was proportional in a certain range of low velocity (<2 mm/s), and that theoretical extraction of oxygen became much lower than transported oxygen in capillaries in the higher velocity range (>2 mm/s). This observation might be explained by thoroughfare channels or non-nutritional capillaries without oxygen exchange in capillaries.

Thoroughfare channels

Our data definitively shows the presence of high flow RBCs in single file channels that have the same diameter size as ordinary capillaries, and therefore can be categorized as 'capillaries' according to our criteria. If the high-flow RBCs are disregarded, the RBC number and average RBC velocity obtained with low frame rate cameras are quite similar to other reports as mentioned above. The high RBC velocity detected here is supported by previous reports in which the calculated RBC velocity was relatively high (1.5 to 2.08 mm/s) when recorded at high frame rate (400 fps) in the cat brain [8, 10]. Yamaguchi et al. detected velocities of approximately 7 mm/s employing a dual window technique with a sampling rate of 200 Hz in combination with the fluorescent flow tracer in cerebral microvessels of cats [11]. Ishikawa et al. measured RBC velocity as 1.0 to 9.0 mm/s in rat pial arteries with an image-intensified high-speed (1000 fps) video camera system [45]. Therefore, RBC velocities tend to be higher as the measuring apparatus improved, coupled with a high-speed camera. The highest value we observed was approximately 16.5 mm/s when we preliminarily measured RBC velocity in the rat cerebral cortex employing a 3000-5000 fps camera laser scanning confocal fluorescence microscope (courtesy of Professor Norio Tanahashi, Department of Neurology, Saitama Medical University, Japan).

High velocity RBCs may be translocating through thoroughfare channels or precapillary arteriovenous anastomoses, which have been observed in the cerebral cortex in dogs [46], humans [47], and rats [48]. Shunting of microspheres through precapillary anastomoses in the brain has been demonstrated in dogs [49-51]. It seems that the capillaries with a high velocity at resting state represent functional thoroughfare channels through which flow may be redistributed to low velocity exchange capillaries to maintain balanced perfusion and transcapillary exchange. Thoroughfare channels may provide a physiological reserve of RBC flow with a minimal change in net capillary flow when cerebral blood supply is challenged. For example, systemic hypotension and severe hypercapnia are accompanied by an increase in the homogeneity of capillary flow, and involves the redistribution of RBC flow between thoroughfare channels and exchange capillaries [14]. The maintenance of flow velocity above a critical value in the slow capillaries could be protection from stasis and leukocyte plugging [52]. RBC velocity appeared autoregulated in the slow flow capillaries (exchange capillary, <1 mm/s) but not in the fast flow capillaries (thoroughfare channels, >1 mm/s) [42]. According to their criteria, extraordinary high flow capillaries detected in the present study may be called thoroughfare channels.

Acknowledgment

The authors thank Otsuka Pharmaceutical Co., Ltd. for their financial support. The KEIO-IS1 and KEIO-IS2 programs are freely available to researchers

in nonprofit organizations; for details, please contact Minoru Tomita at *mtomita@sc.itc.keio.ac.jp*.The authors have no conflict of interest to declare.

References

1. Shepherd GM. The single capillary and the active brain. Proc Natl Acad Sci USA. 2003;100:12535-6.
2. Wayland H, Johnson PC. Erythrocyte velocity measurement in microvessels by a two-slit photometric method. J Appl Physiol. 1967;22:333-7.
3. Tyml K, Ellis CG. Evaluation of the flying spot technique as a television method for measuring red cell velocity in microvessels. Int J Microcirc Clin Exp. 1982;1: 145-55.
4. Kiesewetter H, Radtke H, K rber N, Schmid-Sch nbein H. Experimental calibration of a two-stage prism-grating system for measuring cell velocity. Microvasc Res. 1982;23:56-66.
5. Slaaf DW, Rood JP, Tangelder GJ, Jeurens TJ, Alewijnse R, Reneman RS, et al. A bidirectional optical (BDO) three-stage prism grating system for on-line measurement of red blood cells velocity in microvessels. Microvasc Res. 1981;22:110-22.
6. Rosen B, Paffhausen W. On-line measurement of microvascular diameter and red blood cell velocity by a line-scan CCD image sensor. Microvasc Res. 1993; 45:107-21.
7. Ma YP, Koo A, Kwan HC, Cheng KK. On-line measurement of the dynamic velocity of erythrocytes in the cerebral microvessels in the rat. Microvasc Res. 1974;8:1-13.
8. Pawlik G, Rackl A, Bing RJ. Quantitative capillary topography and blood flow in the cerebral cortex of cats: an in vivo microscopic study. Brain Res. 1981; 208:35-58.
9. Ivanov KP, Kalinina MK, Levkovich YI. Blood flow velocity in capillaries of brain and muscles and its physiological significance. Microvasc Res. 1981;22: 143-55.
10. Chang BL, Santillan G, Bing RJ. Red cell velocity and autoregulation in the cerebral cortex of the cat. Brain Res. 1984;308:15-24.
11. Yamaguchi S, Yamakawa T, Niimi H. Red cell velocity and microvessel diameter measurement by a two fluorescent tracer method under epifluorescence microscopy: application to cerebral microvessels of cats. Int J Microcirc Clin Exp. 1992;11 403-16.
12. Villringer A, Them A, Lindauer U, Einh upl K, Dirnagl U. Capillary perfusion of the rat brain cortex. An *in vivo* confocal microscopy study. Circ Res. 1994;75: 55-62.
13. Hudetz AG. Blood flow in the cerebral capillary network: a review emphasizing observations with intravital microscopy. Microcirculation. 1997;4:233-52.
14. Hudetz AG, Biswal BB, Feh rG, Kampine JP. Effects of hypoxia and hypercapnia on capillary flow velocity in the rat cerebral cortex. Microvasc Res. 1997;54:35-42.
15. Hudetz AG, Feh r G, Kampine JP. Heterogeneous autoregulation of cerebrocortical thoroughfare channels? Microvasc Res 1996;51:131-36.
16. Hudetz AG, Feh rG, Weigle CG, Knuese DE, Kampine JP. Video microscopy of cerebrocortical capillary flow: response to hypotension and intracranial hypertension. Am J Physiol. 1995;268:H2202-10.
17. Hudetz AG, Wood JD, Biswal BB, Krolo I, Kampine JP. Effect of hemodilution on RBC velocity, supply rate, and hematocrit in the cerebral capillary network. J Appl Physiol. 1999;87:505-9.
18. Biswal BB, Hudetz AG. Synchronous oscillations in cerebrocortical capillary red blood cell velocity after nitric oxide synthase inhibition. Microvasc Res. 1996; 52:1-12.
19. Kleinfeld D, Mitra PP, Helmchen F, Denk W. Fluctuations and stimulus-induced changes in blood flow observed in individual capillaries in layers 2 through 4 of rat neocortex. Proc Natl Acad Sci USA. 1998;95:15741-6.
20. Kleinfeld D. Cortical blood flow through individual capillaries in rat vibrissa S1 cortex: stimulus-induced changes in flow are comparable to the underlying fluctuations in flow. In: Tomita M, Kanno K, Hamel E, editors. Brain Activation and CBF Control, International Congress Series 1235: Amsterdam: Elsevier Science; 2002. p. 115-22.
21. Seylaz J, Charbonn R, Nanri K, Von Euw D, Borredon J, Kacem K, et al. Dynamic in vivo measurement of erythrocyte velocity and flow in capillaries and of microvessel diameter in the rat brain by confocal laser microscopy. J Cereb Blood Flow Metab. 1999;19: 863-70.
22. Krolo I, Hudetz AG. Hypoxemia alters erythrocyte perfusion pattern in the cerebral capillary network. Microvasc Res. 2000;59:72-9.
23. Pinard E, Nallet H, MacKenzie ET, Seylaz J, Roussel S. Penumbral microcirculatory changes associated with peri-infarct depolarizations in the rat. Stroke. 2002;33: 606-12.
24. Schulte ML, Wood JD, Hudetz AG. Cortical electrical stimulation alters erythrocyte perfusion pattern in the cerebral capillary network of the rat. Brain Res. 2003;

963:81-92.
25. Chaigneau E, Oheim M, Audinat E, Charpak S. Two-photon imaging of capillary blood flow in olfactory bulb glomeruli. Proc Natl Acad Sci USA. 2003;100: 13081-6.
26. Hutchinson EB, Stefanovic B, Koretsky AP, Silva AC. Spatial flow-volume dissociation of the cerebral microcirculatory response to mild hypercapnia. Neuroimage. 2006;32:520-30.
27. Schiszler I, Takeda H, Tomita M, Tomita Y, Osada T, Unekawa M, Tanahashi N, Suzuki N. Software (KEIO-IS2) for automatically tracking red blood cells (RBCs) with calculation of individual RBC velocities in single capillaries of rat brain (Abstract). J Cereb Blood Flow Metab. 2005;25 (Suppl 1):S541.
28. Tomita M, Osada T, Schiszler I, Tomita Y, Unekawa M, Toriumi H, et al. Automated method for tracking vast numbers of FITC-labeled RBCs in microvessels of rat brain in vivo using a high-speed confocal microscope system. Microcirculation. 2008;15:163-74.
29. Unekawa M, Tomita M, Osada T, Tomita Y and Suzuki N. RBC velocity in intraparenchymal capillaries of the rat brain and its fluctuation. Microcirc Ann. 2005;21: 85-6.
30. Unekawa M, Tomita M, Osada T, Tomita Y, Toriumi H, Suzuki N. Sampling rate-dependent RBC velocity in intraparenchymal single capillaries of rat cerebral cortex. [On line]. Microvasc Rev Commun. 2007;1: 12-5, Available from: http://www.jsmicrocirc.com/mvrc/contents/current/01_01/index.html
31. Unekawa M, Tomita M, Tomita Y, Osada T, Toriumi H, Suzuki N. Extraordinary high flow capillaries in the cerebral microvascular network (Abstract). J Cereb Blood Flow Metab. in press.
32. Hirase H, Creso J, Buzs ki G. Capillary level imaging of local cerebral blood flow in bicuculline-induced epileptic foci. Neuroscience. 2004;128:209-16.
33. Niesner R, Andresen V, Neumann J, Spiecker H, Gunzer M. The power of single and multibeam two-photon microscopy for high-resolution and high-speed deep tissue and intravital imaging. Biophys J. 2007; 93: 2519-29.
34. Theer P, Hasan MT, Denk W. Two-photon imaging to a depth of 1000 microm in living brains by use of a Ti:Al2O3 regenerative amplifier. Opt Lett. 2003;28: 1022-4.
35. Williams JL, Shea M, Jones SC. Evidence that heterogeneity of cerebral blood flow does not involve vascular recruitment. Am J Physiol. 1993;264:H1740-3.
36. Grubbs FE. Testing outlying observations. Ann Mathemat Stat. 1950;21:27-58.
37. Crone C. The permeability of capillaries in various organs as determined by the use of the 'indicator diffusion' method. Acta Physiol Scand. 1963;58: 292-305.
38. Tomita M, Gotoh F. Local cerebral blood flow values as estimated with diffusible tracers: validity of assumptions in normal and ischemic tissue. J Cereb Blood Flow Metab. 1981;1:403-11.
39. Parthasarathi AA, Japee SA, Pittman RN. Determination of red blood cell velocity by video shuttering and image analysis. Ann Biomed Eng. 1999;27:313-25.
40. Japee SA, Pittman RN, Ellis CG. A new video image analysis system to study red blood cell dynamics and oxygenation in capillary networks. Microcirculation. 2005;12:489-506.
41. Japee SA, Pittman RN, Ellis CG. Automated method for tracking individual red blood cells within capillaries to compute velocity and oxygen saturation. Microcirculation. 2005;12:507-15.
42. Hudetz AG. Regulation of oxygen supply in the cerebral circulation. Adv Exp Med Biol. 1997;428:513-20.
43. Hudetz AG, Feh r G, Knuese DE, Kampine JP. Erythrocyte flow heterogeneity in the cerebrocortical capillary network. Adv Exp Med Biol. 1994;345:633-42.
44. Hudetz AG. Mathematical model of oxygen transport in the cerebral cortex. Brain Res. 1999;817:75-83.
45. Ishikawa M, Sekizuka E, Shimizu K, Yamaguchi N, Kawase T. Measurement of RBC velocities in the rat pial arteries with an image-intensified high-speed video camera system. Microvasc Res. 1998;56:166-72.
46. Hasegawa T, Ravens JR, Toole JF. Precapillary arteriovenous anastomoses. "Thoroughfare channels" in the brain. Arch Neurol. 1967;16:217-24.
47. Duvernoy HM, Delon S, Vannson JL. Cortical blood vessels of the human brain. Brain Res Bull. 1981;7: 519-79.
48. Motti ED, Imhof HG, Yasargil MG. The terminal vascular bed in the superficial cortex of the rat. An SEM study of corrosion casts. J Neurosurg. 1986;65:834-46.
49. Kennady JC, Taplin GV. Shunting in cerebral microcirculation. Am Surg. 1967;33:763-71.
50. Marcus ML, Heistad DD, Ehrhardt JC, Abboud FM. Total and regional cerebral blood flow measurement with 7-10-, 15-, 25-, and 50-mum microspheres. J Appl Physiol. 1976;40:501-7.
51. Prosenz P. Investigations on the filter capacity of the dog's brain. A contribution to the question of cerebral arteriovenous shunts. Arch Neurol. 1972;26:479-88.
52. Yamakawa T, Yamaguchi S, Niimi H, Sugiyama I. White blood cell plugging and blood flow maldistribution in the capillary network of cat cerebral cortex in acute hemorrhagic hypotension: An intravital microscopic study. Circ Shock. 1987;22:323-32.